

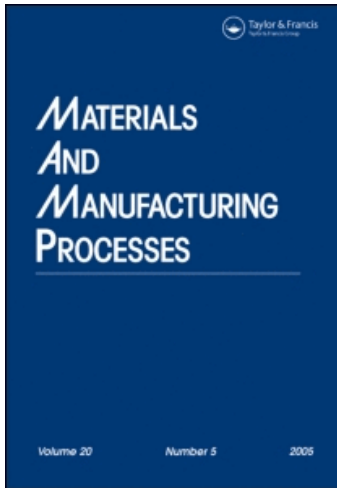
This article was downloaded by: [Tallinn University of Technology]

On: 30 June 2010

Access details: Access Details: [subscription number 907226556]

Publisher Taylor & Francis

Informa Ltd Registered in England and Wales Registered Number: 1072954 Registered office: Mortimer House, 37-41 Mortimer Street, London W1T 3JH, UK



## Materials and Manufacturing Processes

Publication details, including instructions for authors and subscription information:

<http://www.informaworld.com/smpp/title~content=t713597284>

### Nonlinear Acoustic Nondestructive Evaluation (NDE): Qualitative and Quantitative Effects

Jüri Engelbrecht<sup>a</sup>; Arvi Ravasoo<sup>a</sup>; Jaan Janno<sup>a</sup>

<sup>a</sup> Center for Nonlinear Studies, Institute of Cybernetics at Tallinn University of Technology, Tallinn, Estonia

Online publication date: 30 April 2010

**To cite this Article** Engelbrecht, Jüri , Ravasoo, Arvi and Janno, Jaan(2010) 'Nonlinear Acoustic Nondestructive Evaluation (NDE): Qualitative and Quantitative Effects', Materials and Manufacturing Processes, 25: 4, 212 – 220

**To link to this Article:** DOI: 10.1080/10426910903425390

**URL:** <http://dx.doi.org/10.1080/10426910903425390>

PLEASE SCROLL DOWN FOR ARTICLE

Full terms and conditions of use: <http://www.informaworld.com/terms-and-conditions-of-access.pdf>

This article may be used for research, teaching and private study purposes. Any substantial or systematic reproduction, re-distribution, re-selling, loan or sub-licensing, systematic supply or distribution in any form to anyone is expressly forbidden.

The publisher does not give any warranty express or implied or make any representation that the contents will be complete or accurate or up to date. The accuracy of any instructions, formulae and drug doses should be independently verified with primary sources. The publisher shall not be liable for any loss, actions, claims, proceedings, demand or costs or damages whatsoever or howsoever caused arising directly or indirectly in connection with or arising out of the use of this material.

# Nonlinear Acoustic Nondestructive Evaluation (NDE): Qualitative and Quantitative Effects

JÜRI ENGELBRECHT, ARVI RAVASOO, AND JAAN JANNO

Center for Nonlinear Studies, Institute of Cybernetics at Tallinn University of Technology, Tallinn, Estonia

The recent results in constructing the mathematical basis of nonlinear acoustic techniques for nondestructive evaluation (NDE) of inhomogeneous materials are discussed. These include microstructural materials and materials with weakly or strongly changing properties of specimens (structural elements) under inhomogeneous prestress. The idea is to extract additional information from nonlinear and dispersive effects of wave propagation. Novel concepts are introduced: (i) the analysis of dispersive effects; (ii) the analysis of two counter-propagating nonlinear waves.

*Keywords* Dispersion; Inhomogeneity; Microstructure; NDE; Nonlinearity.

## 1. INTRODUCTION

Contemporary materials are usually characterized by their complex structure at various scales. For short, such materials are referred to as “microstructured materials.” These are polycrystalline solids, ceramic composites, functionally graded materials, granular materials, etc. In order to derive mathematical models describing wave propagation in such materials, several theories are proposed by Eringen [1], Mindlin [2], and others, based on continuum theories. The overview of functionally graded materials is given by Suresh and Mortensen [3]. The microstructure brings along dispersive effects in the wave propagation. If we separate macro- and microcontinua in continua [1, 2] then the mathematical models explicitly show the influence of the dispersion due to microstructure. In case the dispersion is balanced by nonlinear effects, solitary waves may emerge. This phenomenon has been analyzed theoretically [4, 5] and also shown in experiments [6]. The analysis shows how phase velocities are dependent on properties of microstructure and how the solitary waves change their shapes in microstructured materials. On the other hand, inhomogeneities of material properties may be described by models with smooth functions describing the averaged changes of density or elastic modulus [7]. Again, if nonlinearities are taken into account, then the wave interaction may change considerably by characteristics of wave fields. In what follows, we give a short overview how dispersive and nonlinear effects can be used for solving the inverse problems, i.e., for nondestructive evaluation (NDE).

## 2. PARAMETERS OF MICROSTRUCTURED MATERIALS

### 2.1. Model Description

There are several models of microstructure, but always the scale-dependence is taken into account [1]. In this

article, we use the Mindlin model [2], where the material is interpreted as an elastic continuum including microstructure that could be “as a molecule of a polymer, a crystallite of a polycrystal, or a grain of a granular material”. This microelement is taken as a deformable cell.

Formalizing one-dimensional deformation processes both in macro- and microscale, one obtains a coupled system of equations of motion that in dimensionless variables reads [8]

$$\begin{aligned} v_{tt} &= a_0 v_{xx} + \frac{\mu}{2} (v^2)_{xx} + \alpha \psi_{xx}, \\ \delta \psi_{tt} &= \delta a_1 \psi_{xx} + \delta^{3/2} \lambda \psi_x \psi_{xx} - \beta v - \gamma \psi. \end{aligned} \quad (2.1)$$

Here,  $v$  is the macrodeformation,  $\psi$  is the microdeformation,  $\delta$  is a geometric parameter related to the scale of the microstructure, and the coefficients  $a_0$ ,  $a_1$ ,  $\alpha$ ,  $\beta$ ,  $\gamma$ ,  $\lambda$ ,  $\mu$  are related to the physical properties of the material.

This system can be simplified by approximation. For instance, using slaving principle, the microdeformation  $\psi$  is eliminated. The result is a Boussinesq-type equation of motion [5, 8]

$$\begin{aligned} v_{tt} &= b v_{xx} + \frac{\mu}{2} (v^2)_{xx} + \delta (\beta_1 v_{tt} - \gamma_1 v_{xx})_{xx} \\ &\quad - \delta^{3/2} \frac{\lambda_1}{2} (v_x^2)_{xxx}, \end{aligned} \quad (2.2)$$

where  $b = a_0 - \frac{\alpha\beta}{\gamma}$ ,  $\beta_1 = \frac{\alpha\beta}{\gamma^2}$ ,  $\gamma_1 = \frac{\alpha\beta a_1}{\gamma^2}$ ,  $\lambda_1 = \frac{\lambda\alpha\beta^2}{\gamma^2}$ .

### 2.2. Using Linear Waves in NDE

We start by NDE of physical parameters  $a_0$ ,  $a_1$ ,  $\alpha$ ,  $\beta$ , and  $\gamma$  of the microstructured material in the linear case when  $\mu = \lambda = 0$ . Then the Fourier transform of the general solution of the basic system (2.1) has the form [9]

$$\begin{aligned} \hat{v}(x, \omega) &= A_+(\omega) e^{ik(\omega)x} + A_-(\omega) e^{-ik(\omega)x}, \\ \hat{\psi}(x, \omega) &= A_+^m(\omega) e^{ik(\omega)x} + A_-^m(\omega) e^{-ik(\omega)x}, \end{aligned} \quad (2.3)$$

Received October 10, 2008; Accepted March 27, 2009

Address correspondence to Jüri Engelbrecht, Center for Nonlinear Studies, Institute of Cybernetics at Tallinn University of Technology, Tallinn, Estonia; E-mail: je@ioc.ee

where  $A_{\pm}^m(\omega) = A_{\pm}(\omega) \left[ \omega^2 - a_0 (k(\omega))^2 \right] \alpha^{-1} (k(\omega))^{-2}$ , and the addends with  $A_+$  and  $A_-$  represent the wave packets propagating to the right and left, respectively. The involved dispersion function

$$k(\omega) = \omega$$

$$\sqrt{\frac{1}{2a_0a_1} \left[ a_0 + a_1 - \frac{a_0\gamma - \alpha\beta}{\delta\omega^2} + \sqrt{\left( a_0 - a_1 - \frac{a_0\gamma - \alpha\beta}{\delta\omega^2} \right)^2 + \frac{4a_1\alpha\beta}{\delta\omega^2}} \right]}$$

is the real solution of the dispersion equation  $\omega^4 + \kappa_1\omega^2k^2 + \kappa_2k^4 + \kappa_3\omega^2 + \kappa_4k^2 = 0$ , where

$$\begin{aligned} \kappa_1 &= -(a_0 + a_1), \quad \kappa_2 = a_0a_1, \\ \kappa_3 &= -\frac{\gamma}{\delta}, \quad \kappa_4 = \frac{a_0\gamma - \alpha\beta}{\delta}. \end{aligned} \tag{2.4}$$

Let the NDE data consist of measurements of the macrodeformation  $v$  in a fixed point of the medium  $x = x_1$  over the time  $t$ . Then we can use the spectrum of  $v(x_1, t)$  and the reconstruction of the unknown parameters is reduced to the following algebraic procedures:

- 1) Extracting the function  $k(\omega)$  from  $\hat{v}(x_1, \omega)$  and computing pairs

$$(\omega_j, k_j), \quad j = 1, \dots, M;$$

- 2) Constructing the linear system

$$\begin{aligned} \kappa_1 \cdot \omega_j^2 k_j^2 + \kappa_2 \cdot k_j^4 + \kappa_3 \cdot \omega_j^2 + \kappa_4 \cdot k_j^2 &= -\omega_j^4, \\ j &= 1, \dots, M \end{aligned} \tag{2.5}$$

on the basis of dispersion equation and solving it for  $\kappa_1, \dots, \kappa_4$ ;

- 3) Solving (2.4) for  $a_0, a_1, \gamma$ , and  $\alpha\beta$ .

In case of normal dispersion (formally, it occurs when the parameters satisfy the inequality  $a_0\gamma - a_1\gamma - \alpha\beta > 0$  (details see [9]) the solution of (2.4) has the form

$$a_0 = \frac{-\kappa_1 + \sqrt{\kappa_1^2 - 4\kappa_2}}{2}, \quad a_1 = \frac{-\kappa_1 - \sqrt{\kappa_1^2 - 4\kappa_2}}{2}, \tag{2.6}$$

$$\gamma = -\delta\kappa_3, \quad \alpha\beta = a_0\gamma - \delta\kappa_4.$$

We remark that it is not possible to separate the parameters  $\alpha$  and  $\beta$  from measurements in macrolevel, because they appear in the product form in all formulas.

The steps 2 and 3 of the presented algorithm are rather straightforward. Step 1 requires more explanation. The functions  $A_+$  and  $A_-$  in the formula of  $\hat{v}(x_1, \omega)$  can be determined by boundary conditions or additional measurements. We consider the simplest physical model when the macrodeformation is specified on the plane  $x = 0$ ,

i.e.,  $v(0, t) = g(t)$ , the packet contains only the waves propagating to the right and the measurement point  $x_1 > 0$ . Then

$$\hat{v}(x_1, \omega) = \hat{g}(\omega) e^{ik(\omega)x_1}. \tag{2.7}$$

We have to solve (2.7) for  $k(\omega)$ . This is a bit complicated due to the periodicity of the outer component  $e^{iz}$  of  $e^{ik(\omega)x_1}$ . Fortunately, the function  $k$  to be determined is strictly increasing. This enables to solve (2.7) by means of the following ideas. The real part of  $e^{ik(\omega)x_1}$  oscillates. Namely, it decreases for  $\omega \in (0, s_1)$ , increases for  $\omega \in (s_1, s_2)$ , and so on, where  $0 < s_1 < s_2 < \dots$  are some numbers. Thus, it is possible to locate the intervals  $(s_n, s_{n+1})$  using the known function  $\text{Re} \frac{\hat{v}(x_1, \omega)}{\hat{g}(\omega)}$ . Thereupon,  $k(\omega)$  can be computed by the formula

$$k(\omega) = \frac{1}{x_1} \left[ (-1)^n \arccos \text{Re} \frac{\hat{v}(x_1, \omega)}{\hat{g}(\omega)} + \pi(n + \theta_n) \right] \text{ for } \omega \in (s_n, s_{n+1}). \tag{2.8}$$

Here  $\theta_n = 0$  for odd  $n$ , and  $\theta_n = 1$  for even  $n$ .

In practice, we have in hand a finite number of measured deformations  $v_l^{\varepsilon} \approx v(x_1, t_l)$ ,  $l = 1, \dots, N$  in a time interval  $[T, T_1]$ , where  $t_l = T + lh$ ,  $h = \frac{T_1 - T}{N}$ , and  $\varepsilon$  is the noise level. We apply the Discrete Fourier Transform (DFT) to compute the discrete spectra

$$\begin{aligned} \hat{g}(\omega_m) &\approx \hat{g}_m = \frac{e^{iT\omega_m}}{N} \sum_{l=0}^{N-1} e^{\frac{2\pi i b l m}{N}} g_{l+1}, \\ \hat{v}(x_1 \omega_m) &\approx \hat{v}_m^{\varepsilon} = \frac{e^{iT\omega_m}}{N} \sum_{l=0}^{N-1} e^{\frac{2\pi i b l m}{N}} v_{l+1}^{\varepsilon} \end{aligned}$$

for  $\omega_m = (m - 1)\tau$ ,  $m = 1, \dots, N$ , where  $\tau > 0$  is the step size in the frequency domain,  $g_l = g((l - 1)h)$  and  $b = \frac{h\tau}{2\pi}$ . By means of the discrete spectra, we compute the sequence  $z_m^{\varepsilon} = \text{Re} \frac{\hat{v}_m^{\varepsilon}}{\hat{g}_m}$ . This sequence oscillates. Namely, it decreases for  $m = s_0, \dots, s_1$ , increases for  $m = s_1, \dots, s_2$ , and so on, where  $1 = s_0 < s_1 < s_2 < \dots$  are some integers. By (2.8), the following formula is valid for wavenumbers:

$$k_m = k(\omega_m) = \frac{1}{x_1} [(-1)^n \arccos z_m + \pi(n + \theta_n)] \text{ for } s_{n-1} < m < s_n. \tag{2.9}$$

Using the latter formula, we compute the pairs  $(\omega_j, k_j)$ ,  $j = 1, \dots, M$  and complete the first step of the algorithm.

*Example problem.* Let us illustrate the described algorithm by means of a numerical example that was solved by means of Mathematica 5.1. We used synthetic data corresponding to the parameters  $a_0 = 10$ ,  $a_1 = \alpha = \gamma = \beta = \delta = 1$  and considered a virtual physical problem with local excitation  $g(t) = e^{-\frac{t^2}{4}}$  at  $x = 0$ . Then  $\hat{g}(\omega) = 2\sqrt{\pi}e^{-\omega^2}$ .

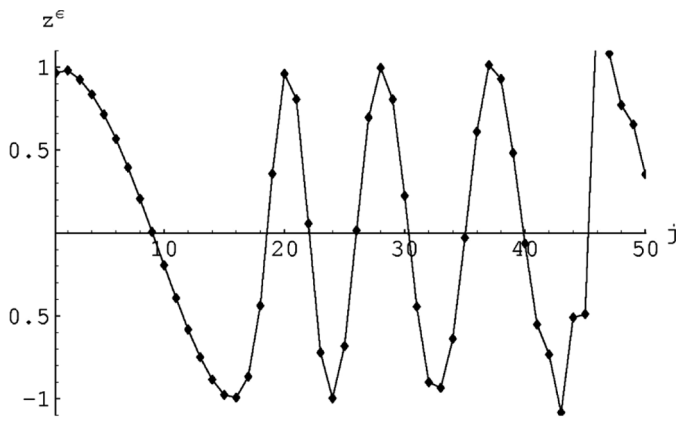


FIGURE 1.—Sequence  $z_m^\epsilon$  for  $m = 1, \dots, 50$ .

The synthetic data were constructed as follows. We evaluated  $v(x_1, t)$  for  $x_1 = 10$  taking inverse Fourier transform of (2.7) numerically by means of Simpson’s rule to guarantee higher accuracy than in DFT. Thereupon, we chose uniform mesh with  $N = 200$  nodes in the time interval  $[-5, 50]$  with the step size  $h = \frac{55}{200}$ . We disturbed the computed deformation values at the nodes by the formula  $v_l^\epsilon = v(-5 + (l - 1)h) + \epsilon R$ ,  $l = 1, \dots, N$ , to obtain the synthetic data. Here,  $\epsilon$  is a given noise level, and  $R$  is the uniformly distributed random number in  $[-1, 1]$ .

Firstly, we solved the problem in case  $\epsilon = 10^{-3}$ . To get the first sight on the situation in frequency domain, we took a larger step size  $\tau = \frac{\pi}{55}$  and computed  $z_m^\eta = \text{Re} \frac{\hat{v}_m^\epsilon}{\hat{g}_m}$ . (Figure 1; for comparison, exact  $\cos[k(\omega)x_1]$  is given in Fig. 2.) Clearly,  $z_m^\epsilon$  is oscillating with critical numbers  $s_0 = 0, s_1 = 16, s_2 = 20, s_3 = 24, \dots$ . Higher disturbance occurs from the fourth period because of the very small denominator  $\hat{g}_m$  ( $\hat{g}(\omega)$  is rapidly decreasing). To guarantee maximal accuracy, we truncated the subrange  $\omega > 2$  and computed new values of the spectra with the smaller step size  $\tau = \frac{1}{200}$  in order to remain inside the interval  $\omega \in (0, 2)$ . By means of (2.9), we constructed data for the system (2.5), solved it by least squares, and computed the parameters using (2.6). The result was  $a_0^\epsilon = 9.97, a_1^\epsilon = 1.002, \lambda^\epsilon = 0.995, (\alpha\beta)^\epsilon = 0.975$ . Then we repeated

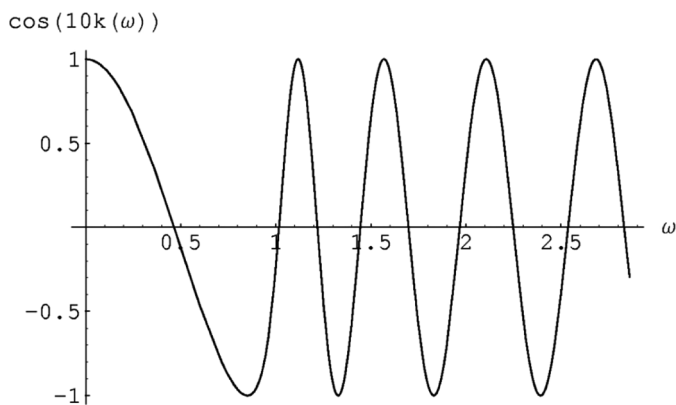


FIGURE 2.—Function  $\cos[k(\omega)x_1]$  in case  $x_1 = 10$ .

the solution procedure 50 times taking different random numbers  $R$  with the same noise level  $\epsilon = 10^{-3}$ . The biggest relative errors in  $a_0, a_1, \gamma$ , and  $\alpha\beta$  were 0.6%, 0.4%, 1.0%, and 5.2%, respectively. Moreover, we solved the problem for the noise level  $\epsilon = 10^{-2}$  for 50 cases of random  $R$ , too. Then the biggest relative errors were 3.6%, 2.2%, 1.7%, and 35%, respectively. The numerical results show that the product  $\alpha\beta$  is much more sensitive with respect to the noise than other physical parameters.

### 2.3. Using Solitary Waves in NDE

Now we return to the approximate nonlinear Eq. (2.2). It contains two hierarchical wave operators  $v_{tt} - bv_{xx} + \frac{\mu}{2}(v^2)_{xx}$  and  $\beta_1 v_{ttxx} - \gamma_1 v_{xxxx} - \delta^{1/2} \frac{\lambda_1}{2}(v_x^2)_{xxx}$ , corresponding to macro- and microscale, respectively [8, 9]. We are interested in the reconstruction of the pair  $P = (b, \mu)$  and the triplet  $T = (\beta_1, \gamma_1, \lambda_1)$  of parameters corresponding to these scales. As we will see later on, the methods to determine  $P$  and  $T$  are quite different.

Usage of general nonlinear waves in NDE is a rather complicated task. Therefore, we will be limited to simpler waveforms, namely, solitary waves. Equation (2.2) possesses bell-shaped asymmetric solitary wave solutions  $v(x, t) = w(x - ct)$  for velocities  $c$  satisfying the inequality  $\left(\frac{\beta_1 c^2 - \gamma_1}{c^2 - b}\right)^3 > \frac{4\lambda_1^2}{\mu^2}$  [5], and the wave shape  $w = w(\xi)$  solves the following ordinary differential equation (ODE):

$$(w')^2 - \Theta(w')^3 = \kappa^2 w^2 \left(1 - \frac{w}{A}\right), \tag{2.10}$$

where

$$\begin{aligned} \kappa &= \sqrt{\frac{c^2 - b}{\delta(\beta_1 c^2 - \gamma_1)}}, \\ A &= \frac{3(c^2 - b)}{\mu}, \\ \Theta &= \frac{2\delta^{1/2}\lambda_1}{3(\beta_1 c^2 - \gamma_1)}. \end{aligned} \tag{2.11}$$

Here  $A$  is the amplitude,  $\kappa$  is the exponential decay rate, i.e.,  $w \sim e^{-\kappa|\eta|}$  as  $|\eta| \rightarrow \infty$ , and  $\Theta$  is related to the asymmetry. The direction of asymmetry depends on the sign of  $\Theta$  (Figs. 3 and 4).

We remark that a single solitary wave does not contain enough information to recover all five unknowns  $b, \mu, \beta_1, \gamma_1, \lambda_1$ . The reason is that it has only three degrees of freedom:  $A, \kappa$ , and  $\Theta$ . Therefore, let us have two waves,  $w[c_1]$  and  $w[c_2]$ , with the velocities  $c_1$  and  $c_2$ , satisfying  $c_1^2 \neq c_2^2$ , and the amplitudes  $A_1$  and  $A_2$ , respectively. From the formula of  $A$  in (2.14) we deduce the simple linear system  $3b + A_j \mu = 3c_j^2, j = 1, 2$ , for the pair of unknowns  $P = (b, \mu)$ .

However, amplitudes do not contain any information about the triplet  $T = (\beta_1, \gamma_1, \lambda_1)$ . To determine  $T$ , we use half lengths of waves measured at some given levels.

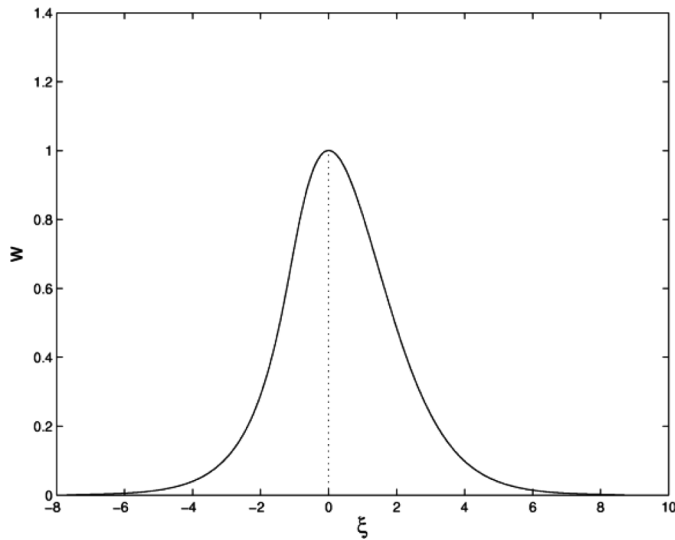


FIGURE 3.—Solitary wave in case  $A = \kappa = 1, \Theta = 0.9$ .

More precisely, let us fix a number  $w_1$  which lies between 0 and  $A_1$ , and a number  $w_2$  which lies between 0 and  $A_2$ . Concerning the first wave, we register the time when it attains the level  $w_1$ , the extremum  $w = A_1$ , and the time when it drops below the level  $w_1$ . Using the velocity  $c_1$ , we can then compute the relative coordinates  $\xi = \xi_{1l} > 0$  and  $\xi = \xi_{1l} < 0$ , such that  $w[c_1](\xi_{1l}) = w_1, l = 1, 2$  (i.e., front and rear half lengths). Similarly, for the second wave  $w[c_2]$ , we register the time when it attains the level  $w_2$ . Then, using the arrival time of the extremum  $w = A_2$  and the velocity  $c_2$ , we can compute  $\xi_2 > 0$  such that  $w[c_2](\xi_2) = w_2$  (front half length).

It was shown in [10] that the data  $\xi_{11}, \xi_{12}, \xi_2$  uniquely recover the triplet  $T$ . The problem for  $T$  is the  $3 \times 3$

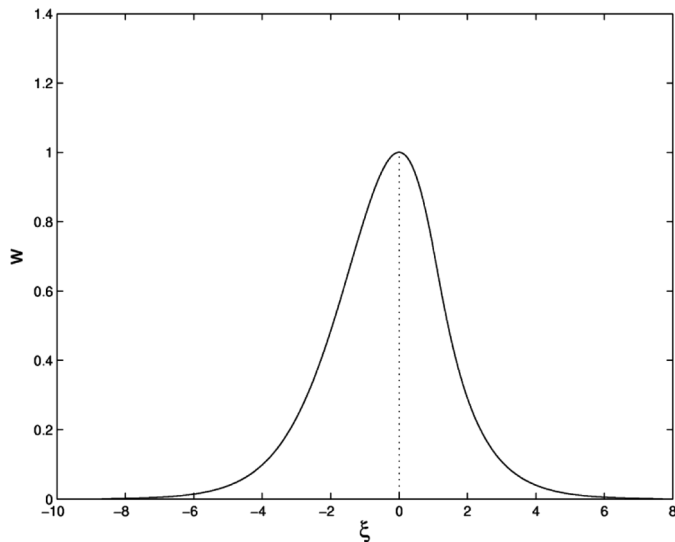


FIGURE 4.—Solitary wave in case  $A = \kappa = 1, \Theta = -0.9$ .

nonlinear system of equations

$$\begin{aligned} w[T, c_1](\xi_{11}) - w_1 &= 0, \\ w[T, c_1](\xi_{12}) - w_1 &= 0, \\ w[T, c_2](\xi_2) - w_2 &= 0. \end{aligned} \tag{2.12}$$

Here,  $T$  in the square brackets points the dependence of  $w$  on  $T$  out. The system (2.12) can be solved by gradient- or Newton-type methods. Then in every step of the method one has to solve twice the ODE (2.10) to determine  $w[T, c_1], w[T, c_2]$ , and additional 9 ODE-s to determine components of the Jacobian matrix of (2.12).

We will present a simpler reconstruction algorithm that avoids solution of ODE-s in the iteration. Let us denote by  $\xi^+[T, c](w)$  and  $\xi^-[T, c](w)$  the inverses of the function  $w[T, c](\xi)$  in the subintervals  $\xi > 0$  and  $\xi < 0$ , respectively. These inverses have the following formula [10]:

$$\xi^\pm[T, c](w) = \frac{1}{\kappa} f^\pm[\rho](w), \tag{2.13}$$

where  $\rho = \Theta\kappa = \frac{2\lambda_1}{3(\beta_1 c^2 - \gamma_1)} \sqrt{\frac{c^2 - b}{\beta_1 c^2 - \gamma_1}}$ , the functions  $f[\rho] = f^\pm[\rho]$  admit the following representations:

$$f[\rho](w) = s_0 I_0(w) + \rho \sum_{i=1}^{\infty} s_i \rho^{i-1} I_i(w) \tag{2.14}$$

with

$$I_i(w) = \begin{cases} -2 \ln \left[ \sqrt{\frac{A}{w}} \left( 1 + \sqrt{1 - \frac{w}{A}} \right) \right] & \text{if } i = 0 \\ 2A^i \sum_{j=0}^{i-1} \binom{i-1}{j} (-1)^{j+1} \frac{\left(1 - \frac{w}{A}\right)^{\frac{i+1}{2} + j}}{i + 2j + 1} & \text{if } i \geq 1 \end{cases},$$

and coefficients  $s_i$  in (2.17) are computed by the recursive formulas

$$\begin{aligned} s_0 &= \pm 1, \quad s_1 = (1 - 3s_0^2)^{-1}, \\ s_i &= (1 - 3s_0^2)^{-1} \sum_{\substack{0 \leq i_1, i_2, i_3 < i \\ i_1 + i_2 + i_3 = i}} s_{i_1} s_{i_2} s_{i_3} \quad i \geq 2. \end{aligned}$$

Here the sequences starting with  $s_0 = -1$  and  $s_0 = 1$  lead to the functions  $f^+[\rho]$  and  $f^-[\rho]$ , respectively. To compute  $f^\pm[\rho_j]$  practically, one can truncate the series in (2.14).

Thus, the nonlinear system (2.12) can be rewritten in the following form:

$$f^+[\rho_1](w_1) - \xi_{11} \kappa_1 = 0, \tag{2.15}$$

$$f^-[\rho_1](w_1) - \xi_{12} \kappa_1 = 0,$$

$$f^+[\rho_2](w_2) - \xi_2 \kappa_2 = 0, \tag{2.16}$$

where  $\rho_j, \kappa_j$  are related to the triplet  $T = (\beta_1, \gamma_1, \lambda_1)$  by the expressions

$$\rho_j = \frac{2\lambda_1}{3(\beta_1 c_j^2 - \gamma_1)} \sqrt{\frac{c_j^2 - b}{\beta_1 c_j^2 - \gamma_1}}, \quad (2.17)$$

$$\kappa_j = \frac{2\lambda_1}{3(\beta_1 c_j^2 - \gamma_1)} \sqrt{\frac{c_j^2 - b}{\delta(\beta_1 c_j^2 - \gamma_1)}}, \quad j = 1, 2.$$

Summing up, the algorithm to reconstruct  $T$  consists of the following steps:

- 1) Solving the  $2 \times 2$  nonlinear subsystem (2.15) for the unknowns  $\rho_1$  and  $\kappa_1$ ;
- 2) Computing the parameter  $\lambda_1$ , and expressing  $\kappa_2$  in terms of  $\rho_2$  by means of the formulas  $\lambda_1 = \frac{3(c_1^2 - b)\rho_1}{2\delta^{3/2}\kappa_1^3}$  and  $\kappa_2 = \left[\frac{3(c_2^2 - b)}{2\delta^{3/2}\lambda_1}\rho_2\right]^{1/3}$  deduced from (2.17);
- 3) Substituting the obtained formula of  $\kappa_2$  into (2.16), and solving the resulting equation

$$f^+[\rho_2](w_2) - \xi_2 \left[ \frac{3(c_2^2 - b)}{2\delta^{3/2}\lambda_1} \right]^{1/3} \rho_2^{1/3} = 0 \quad (2.18)$$

for  $\rho_2$ ;

- 4) Computing  $\beta_1$  and  $\gamma_1$  by means of solution of the linear system

$$\beta_1 c_1^2 - \gamma_1 = \frac{c_1^2 - b}{\delta \kappa_1^2}, \quad (2.19)$$

$$\beta_1 c_2^2 - \gamma_1 = \left[ \frac{4\lambda_1^2 (c_2^2 - b)}{9\rho_2^2} \right]^{1/3}$$

deduced from (2.17).

We emphasize that (2.15) contains sums of functions of single variables  $\rho_1$  and  $\kappa_1$ . This enables to apply the method of secants to solve the system (2.15), hence one has no need to compute derivatives in the iteration process.

*Numerical example.* We solved a problem with synthetic data corresponding to parameters  $\delta = 1, \mu = 6, b = 2, T = (\beta_1, \gamma_1, \lambda_1) = (2, 6, 2.5)$  and virtual waves with velocities  $c_1 = 2, c_2 = 2.2$ . Then  $A_1 = 1, A_2 = 1.42, \kappa = 1, \rho_1 = 0.83333, \kappa_2 = 1.04933, \rho_2 = 0.39787$ . In both waves, we chose the measurement level  $A/2$  for the half lengths. Then,  $w_1 = 0.5$  and  $w_2 = 0.71$ , and the related half lengths (i.e., synthetic data) are  $\xi_{11} = 3.47336, \xi_{12} = 3.27119$ , and  $\xi_3 = 3.45582$ .

To solve the system (2.18), we applied the method of secants with the initial guesses  $\rho_1^0 = 0, \rho_1^1 = 0.1, \kappa_1^0 = \kappa_1^1 = 5$  and truncated the series (2.14) at  $i = 10$ . The method gave a solution with accuracy of 0.001 after 7 steps of iteration. To solve (2.18), we chose the initial guesses  $\rho_2^0 = 0.5, \rho_2^1 =$

0.6, and applied also the method of secants. We reached a solution with the accuracy of 0.001 after 5 steps of iteration. Summing up, 12 steps of iteration were needed to compute the solution of the inverse problem with the accuracy of 0.001.

### 3. SMOOTH INHOMOGENEITIES AND WAVE INTERACTION

Inhomogeneities, evoked by averaged changes of material properties (density, linear, and nonlinear elasticity) or by external forces, may be described by models with smooth functions [7] resorting to the nonlinear theory of elasticity [1]. Similarly to the case with discrete microstructure (see above), the determination of physical properties needs enhanced algorithms. Therefore, the interest is directed to elaboration of extended techniques for ultrasonic NDE of material properties by exploiting the nonlinear effects of wave propagation and the wave interaction in such inhomogeneous materials. Proposed algorithms are based on through transmission techniques for NDE of weakly variable properties of physically inhomogeneous nonlinear elastic material [10] and for inhomogeneously prestressed materials (structural elements) [11]. The wave interaction resonance technique is elaborated for NDE of the properties of weakly inhomogeneous material [12, 13]. The recent results in constructing the mathematical basis of nonlinear wave interaction techniques for NDE of inhomogeneous prestress in the material are described in more detail below.

#### 3.1. Governing Equations

Plates, beams, thin-walled structures, etc. are widely used in civil engineering. The material of these structures is itself isotropic and homogeneous, but inhomogeneity is introduced by prestress. In most applications, deformations of structures are small but finite and, theoretically, they are described by the five constant nonlinear theory of elasticity [1] with geometrical nonlinearity also taken into account. The important thing is that most of these structures have two parallel boundaries. This leads to the idea of using the interaction of waves, evoked simultaneously on opposite boundaries for NDE of the state of the material of structure. It is obvious that the counter-propagation and the interaction of waves involve more information about material properties than it may be obtained by the through transmission technique.

The problem is investigated as follows. A specimen (structural element) with two parallel boundaries is considered. Three states of the material of the specimen are distinguished. The initial state of it corresponds to the undeformed natural state. At the instant  $t = 0$ , the specimen is subjected to the external forces and, furthermore, it is deformed. At the instant  $t = t_0 > 0$ , the wave process in the prestressed specimen is excited. The components of the displacement vector at this present state  $U_K^*(X_J, t)$  are expressed by the formula

$$U_K^*(X_J, t) = U_K^0(X_J, t) + U_K(X_J, t), \quad (3.20)$$

where displacements  $U_K^0(X_J, t)$  and  $U_K(X_J, t)$  are caused by prestress and wave motion, correspondingly.

The equation of motion of the specimen at the present state has the form

$$[T_{KL}^*(X_J, t) (\delta_{KL} + U_{k,L}^*(X_J, t))]_{,K} - \rho_0 U_{k,tt}^*(X_J, t) = 0, \tag{3.21}$$

where  $\delta_{KL}$  denotes the Kroneker delta,  $T_{KL}$  the Kirchhoff pseudostress tensor,  $\rho_0$  the density of the material,  $x_K$  the Eulerian rectangular coordinate, and  $t$  the time.

The case of plane strain is studied, and the components of displacement vector  $U_3^*(X_J, t)$  and  $U_3^0(X_J, t)$  are taken equal to zero. After the instant  $t = 0$ , the specimen is undergoing the static prestress, and the equilibrium of it is described by a system of two elliptic second-order partial differential equations

$$\begin{aligned} & [1 + k_1 U_{I,I}^0(X_1, X_2) + k_2 U_{J,J}^0(X_1, X_2)] U_{I,I}^0(X_1, X_2) \\ & + [2 + k_3 U_{I,J}^0(X_1, X_2) + 2k_4 U_{J,I}^0(X_1, X_2)] U_{I,IJ}^0(X_1, X_2) \\ & + [k_7 + k_3 U_{I,I}^0(X_1, X_2) + k_3 U_{J,J}^0(X_1, X_2)] U_{I,JJ}^0(X_1, X_2) \\ & + [k_4 U_{I,J}^0(X_1, X_2) + k_3 U_{J,I}^0(X_1, X_2)] U_{J,II}^0(X_1, X_2) \\ & + [k_3 U_{I,J}^0(X_1, X_2) + k_4 U_{J,I}^0(X_1, X_2)] U_{J,JJ}^0(X_1, X_2) \\ & + [k_6 + k_5 U_{I,I}^0(X_1, X_2) + k_5 U_{J,J}^0(X_1, X_2)] \\ & \times U_{J,JI}^0(X_1, X_2) = 0. \end{aligned} \tag{3.22}$$

Here, indices  $I = 1, J = 2$  specify the first equation, and  $I = 2, J = 1$  the second equation. The coefficients  $k_l, l = 1, 2, \dots, 7$  characterize the properties of the nonlinear elastic material [7].

Introducing Eq. (3.20) into Eq. (3.21), and taking into account the equations of equilibrium (3.22), the equation that governs the quasi-one-dimensional problem of longitudinal wave propagation in two-dimensional specimen yields

$$\begin{aligned} & [1 + f_1(X_1, X_2)] + U_{1,11}(X_1, X_2, t) \\ & + f_2(X_1, X_2) U_{1,1}(X_1, X_2, t) \\ & + f_3 U_{1,1}(X_1, X_2, t) U_{1,11}(X_1, X_2, t) \\ & - c^{-2} U_{1,tt}(X_1, X_2, t) = 0. \end{aligned} \tag{3.23}$$

The coordinate  $X_2$  may be regarded here as a parameter. Coefficients of the equation

$$\begin{aligned} f_1(X_1, X_2) &= k_1 U_{1,1}^0(X_1, X_2) + k_2 U_{2,2}^0(X_1, X_2), \\ f_2(X_1, X_2) &= k_1 U_{1,11}^0(X_1, X_2) \\ &+ k_3 U_{1,22}^0(X_1, X_2) (k_2 + k_4) U_{2,21}^0(X_1, X_2), \\ f_3 &= k_1, \quad c^{-2} = \rho_0 k \end{aligned} \tag{3.24}$$

are dependent on the prestress and the properties of the material.

### 3.2. Solution Procedure

The wave process in the prestressed material is governed by Eq. (3.23). To solve this equation, it is necessary to determine the coefficients (3.24), i.e., to have some preliminary information about the prestressed state of the specimen. This information may be obtained from the observation data of the loading scheme of the specimen (structural element). Here the problem is solved by assumption that the type of prestressed state and the physical properties of the material are known, and the coefficients of the equation of motion (3.23) are known functions that involve unknown parameters of the prestressed state. Theoretically, these coefficients are determined by the solution to Eqs. (3.22). The perturbative analytical solution in the form of series

$$U_K^0(X_1, X_2) = \sum_{m=1}^{\infty} \varepsilon^m U_K^{0(m)}(X_1, X_2) \tag{3.25}$$

with the small parameter  $|\varepsilon| \leq 1$  is derived for the special case of prestress that corresponds to the pure bending with compression or tension. Introducing series (3.25) into Eqs. (3.22), the system of equations for determination of terms in series (3.25) follows. Up to now, there is an analytical solution to Eqs. (3.22) in our possession. This means that now it is possible to solve Eq. (3.23) with known space dependent variable coefficients.

The perturbation technique is used, and the solution to Eq. (3.23) is sought in the form

$$U_1(X_1, X_2, t) = \sum_{n=1}^{\infty} \varepsilon^n U_1^{(n)}(X_1, X_2, t). \tag{3.26}$$

Introducing series (3.25) and (3.26) with small parameter  $\varepsilon$  into Eq. (3.23), and following the perturbation procedure, a set of equations to determine the terms in series (3.26) yields. Equation (3.23) is solved under the initial and boundary conditions

$$\begin{aligned} U_1(X_1, X_2, 0) &= U_{1,t}(X_1, X_2, 0) = 0, \\ U_{1,t}(0, X_2, t) &= \varepsilon a_0 \varphi(t) H(t), \\ U_{1,t}(h, X_2, t) &= \varepsilon a_h \psi(t) H(t). \end{aligned} \tag{3.27}$$

Here  $H(t)$  denotes Heaviside's unit step function,  $a_0$  and  $a_h$  are constants, and  $h$  denotes the thickness of the specimen. The smooth arbitrary initial wave profiles are determined by functions  $\varphi(t)$  and  $\psi(t)$  with  $\max |\varphi(t)| = 1$  and  $\max |\psi(t)| = 1$ .

The obtained analytical solution, which is too cumbersome to be presented here, describes the initial stage of counter-propagation of waves with arbitrary smooth initial profiles.

### 3.3. Using Wave Interaction in NDE

The intention is to solve the problem of NDE of material inhomogeneity (prestress) on the basis of data about counter-propagation and interaction of waves in the

specimen. Therefore, harmonic waves ( $\varphi(t) = \psi(t) = \sin \omega t$ , where  $\omega$  denotes the frequency) with the same amplitude and frequency, are excited on the opposite boundaries of the specimen in terms of particle velocity. The distorted wave profiles are recorded on the same boundaries in term of stress. The recorded data are analyzed resorting to the perturbative solution (3.26) that makes it possible to separate the linear and nonlinear effects of counter-propagation of harmonic waves.

The dimensionless second term  $U_{1,1}^{(2)}(X_1, X_2, t)$  describes the main domain of nonlinear effects including the evolution of the second harmonic, influence of the prestress to the evolution of the first harmonic, nonlinear interaction between two first harmonics, and influence of the nonlinear physical properties of the material on the wave propagation (Fig. 5).

For an example, the material of the specimen is chosen to be duralumin with density  $\rho_0 = 2800 \text{ kg/m}^3$ , constants of elasticity

$$\begin{aligned} \lambda &= 50 \text{ GPa}, & \mu &= 27.6 \text{ GPa}, \\ \nu_1 &= -136 \text{ GPa}, & \nu_2 &= -197 \text{ GPa}, & \nu_3 &= -38 \text{ GPa}, \end{aligned}$$

and thickness  $h = 0.1 \text{ m}$ . The strain is characterized by the dimensionless constant  $\varepsilon$  that is proposed to be equal to  $\varepsilon = 1 * 10^{-4}$ . The prestressed state of the medium corresponds to the plane strain characterized by the component  $T_{22}^0 = 1 + bX_1$  of the Kirchhoff pseudostress tensor.

Two longitudinal sine waves with the frequency  $\omega = 1.9256 * 10^6 \text{ rad/s}$  are excited simultaneously in the material according to the boundary conditions (3.27). The recorded data contain maximum information about the prestressed state provided the strain intensities caused by the prestress and the wave motions are of the same order [7]. To assure this the amplitude of the excited particle velocity at the boundaries  $X_1 = 0$  and  $X_1 = h$  has the opposite sign  $a_0 = -a_h = -c \text{ m/s}$  and the equal absolute value  $|\varepsilon a_0| = 0.6130 \text{ m/s}$ .

Analysis of numerous numerical experiments leads to the conclusion that the amplitude of boundary oscillations is

dependent on the physical properties of the material and on the parameters and nature of the prestress (inhomogeneity).

**3.3.1. Qualitative NDE.** Further, the possibility of NDE of the two-parametric prestressed state of the specimen on the basis of nonlinear distortion of the wave profile of the initially harmonic wave is discussed. It is assumed that there is an access to two parallel traction free boundaries of the specimen. The problem is studied theoretically. In our possession is the analytical expression for the function  $U_{1,1}(X_1, X_2, t)$  on the whole  $X_1/h, t/\tau$  plane. Therefore, it is possible to describe and analyze the wave propagation, interaction, and evolution of nonlinear effects of wave propagation in any section of the specimen. Due to the complexity of the analytical solution, oscillations on the boundaries are studied numerically.

The nonlinear theory of elasticity [1] describes the stress as a function of the derivatives of the particle displacement with respect to the spatial coordinates. This is the reason why, henceforth, the influence of the prestress on the wave profile is discussed on the basis of function  $U_{1,1}(X_1, X_2, t)$  derived from the solution (3.26):

$$U_{1,1}(X_1, X_2, t) = \sum_{n=1}^{\infty} \varepsilon^n U_{1,1}^{(n)}(X_1, X_2, t). \quad (3.28)$$

The point of discussion is the following: Is it possible qualitatively to distinguish the special cases of the prestressed states of elastic material on the basis of longitudinal wave profile distortion data recorded simultaneously on parallel surfaces of the specimen?

The considered two-parametric prestressed state of the specimen enables to study the wave profile distortion in:

- (i) Homogeneous prestress-free nonlinear elastic material ( $T_{22}^0(X_1) = 0$ );
- (ii) Homogeneously prestressed nonlinear elastic material ( $T_{22}^0(X_1) = a$ );
- (iii) Nonlinear elastic material undergoing pure bending ( $T_{22}^0(0) = -T_{22}^0(h)$ );
- (iv) Nonlinear elastic material undergoing pure bending with tension or compression ( $T_{22}^0(X_1) = a + bX_1$ ).

Prevalent part of the influence of prestress, the physical and geometrical nonlinearity on wave process is described by the second term  $U_{1,1}^{(2)}(X_1, t)$  in series (3.28). The evolution of the prevalent part of nonlinear effects is characterized on the boundaries  $X_1 = 0$  and  $X_1 = h$  of the prestress-free nonlinear material by the oscillations with the double frequency  $2\omega$  and by the constant amplitudes in the interval of propagation and in the interval of interaction.

The presence of homogeneous prestress in the material is characterized by the modulation of boundary oscillation amplitudes. The amplitude and the depth of modulation are dependent on the value and the sign (compression or tension) of prestress. The homogeneity of the prestress is specified by the coincidence of oscillation profiles on the boundaries  $X_1 = 0$  and  $X_1 = h$ .

The inhomogeneous prestress (bending of the sample, for example) involves disparity in oscillation profiles on the

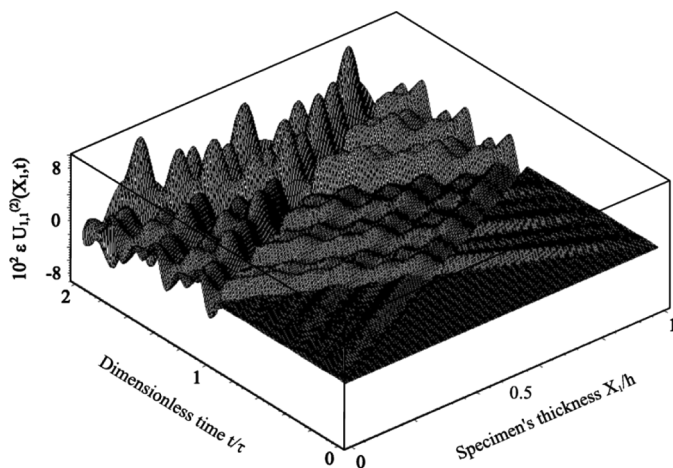


FIGURE 5.—Nonlinear effects of wave interaction.

boundaries  $X_1 = 0$  and  $X_1 = h$ . Exception is the case of pure bending ( $T_{22}^0(0) = -T_{22}^0(h)$ ), when oscillations on both boundaries coincide with phase shift. Consequently, the qualitative effects of boundary oscillation profile distortion enable easily to determine qualitatively the presence and the nature of prestress and to distinguish (i) prestress free material, (ii) homogeneously prestressed material, (iii) material undergoing pure bending, and (iv) material undergoing pure bending with tension or compression.

3.3.2. *Quantitative NDE.* The problem of quantitative nondestructive characterization of two-parametric prestress field is solved by the assumption that the geometry and the physical properties of the material (structural element) are known. The derived analytical solution (3.28) is used, and the plots nonlinear oscillations on the boundaries of the prestress free material are composed. Two first local maxima of the boundary oscillations are determined and characterized by the values of dimensionless instants  $\tau_1$  and  $\tau_2$  (Fig. 6).

The next step is to compose plots boundary oscillation amplitudes vs. prestress parameters  $a$  and  $b$  for both instants  $\tau_1$  (Fig. 7) and  $\tau_2$ . In order to evaluate the unknown values of prestress parameters  $a$  and  $b$  in a physical experiment, the counterpropagating harmonic waves are excited in the specimen undergoing pure bending with tension or compression and the oscillation profiles are recorded on both boundaries. The difference of the values of oscillation amplitudes on opposite boundaries is determined for both instants  $\tau_1$  and  $\tau_2$ . Resorting to the corresponding plots, two possible values of the parameter  $b$  are determined making use of the calculated differences. The value of the parameter  $a$  and the final value of the parameter  $b$  are determined making use of the value of the recorded oscillation amplitude on one of the boundaries at the instant  $\tau_1$  or  $\tau_2$ .

4. SUMMARY

In order to enhance the accuracy of NDE, mathematical modeling must have a proper and sound basis. Here

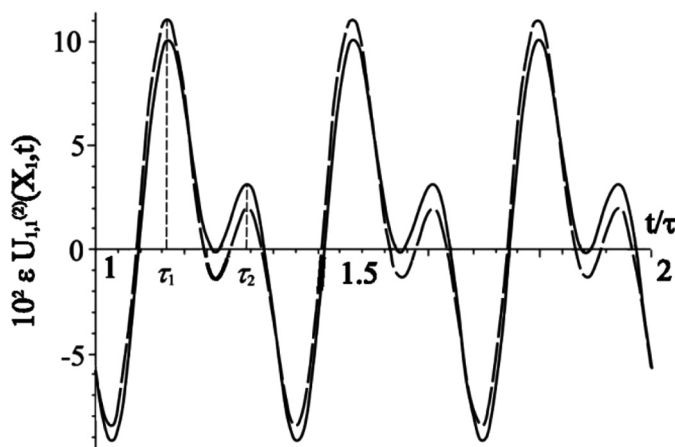


FIGURE 6.—Oscillations on parallel boundaries (line —  $X_1 = 0$ , dashed line -.-.  $X_1 = h$ ).

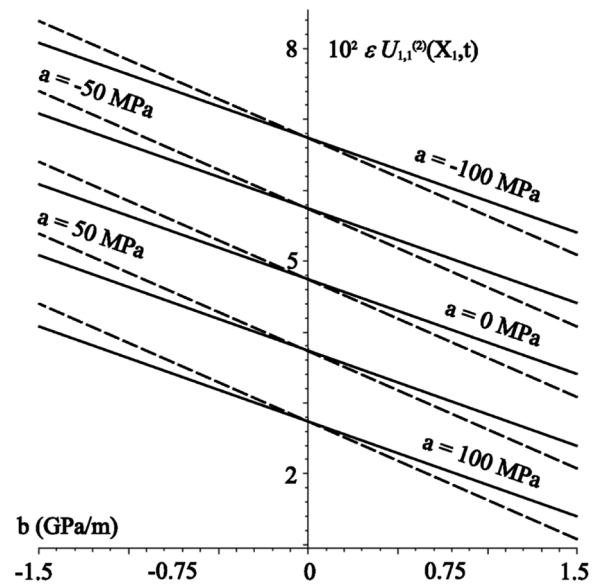


FIGURE 7.—Boundary oscillation amplitudes versus prestress parameters at the instant  $\tau_1$  (line —  $X_1 = 0$ , dashed line -.-.  $X_1 = h$ ).

our models are based on nonlinear continuum theories. The examples shown are one-dimensional or quasi-one-dimensional. In practical realization, however, ultrasonic transducers generate wave beams for which the diffractive expansion in the transverse direction is rather weak. On the axis of the wave beam, the one-dimensional approximation is possible [14].

ACKNOWLEDGMENT

The work was supported by the Estonian Science Foundation (Grant No. 6018).

REFERENCES

1. Eringen, A.C. *Microcontinuum Field Theories I. Foundations and Solids*; Springer: New York, 1999; 348 pp.
2. Mindlin, R.D. Micro-structure in linear elasticity. *Arch. Rat. Mech. Anal.* **1964**, *16*, 51–78.
3. Suresh, S.; Mortensen, A. *Fundamentals of Functionally Graded Materials*; IOM Comm. Ltd.: London, 1998; 166 pp.
4. Porubov, A.V.; Pastrone, F. Non-linear bell-shaped and kink-shaped strain waves in microstructured solids. *Int. J. Non-Linear Mech.* **2004**, *39*, 1289–1299.
5. Janno, J.; Engelbrecht, J. Solitary waves in nonlinear microstructured materials. *J. Phys. A: Math. Gen.* **2005**, *38*, 5159–5172.
6. Potapov, A.I.; Rodyushkin, V.M. Experimental study of strain waves in materials with a microstructure. *Acoust. Phys.* **2001**, *47*, 347–352.
7. Ravasoo, A.; Braunbrück, A. nonlinear acoustic techniques for NDE of materials with variable properties. In *Universality of Nonclassical Nonlinearity. Applications to Non-Destructive Evaluations and Ultrasonics*; Delsanto, P.P., Ed.; Springer, New York, 2007, 425–442.
8. Engelbrecht, J.; Berezovski, A.; Pastrone, F.; Braun, M. Waves in microstructured materials and dispersion. *Phil. Mag.* **2005**, *85*, 4127–4141.

9. Janno, J.; Engelbrecht, J. Inverse problems related to a coupled system of microstructure. *Inverse Problems* **2008**, *24*, 1–15.
10. Ravasoo, A. Nonlinear waves in characterization of inhomogeneous elastic material. *Mechanics of Materials* **1999**, *31*, 205–213.
11. Ravasoo, A. Ultrasonic nondestructive evaluation of inhomogeneous plane strain in elastic medium. *Res. Nondestr. Eval.* **1995**, *7*, 55–68.
12. Braunbrück, A.; Ravasoo, A. Nonlinear interaction and resonance of counterpropagating waves. *Int. J. Pure Appl. Math.* **2008**, *42* (2), 205–215.
13. Ravasoo, A. Non-linear interaction of waves in prestressed material. *Int. J. Non-Linear Mech.* **2007**, *42*, 1162–1169.
14. Achenbach, J.D. *Wave Propagation in Elastic Solids*; NHPC: Amsterdam, 1973; 425 pp.